控制与决策
Control and Decision

输出死区下的随机多智能体系统一致性饱和控制

于跃飞, 林国怀, 马慧, 周琪, 鲁仁全

引用本文:
于跃飞,林国怀,马慧,周琪,鲁仁全. 输出死区下的随机多智能体系统一致性饱和控制[J]. 控制与决策, 2023, 38(5): 1249-1257.

在线阅读 View online: https://doi.org/10.13195/j.kzyjc.2022.0296

您可能感兴趣的其他文章

Articles you may be interested in

基于神经网络逼近的异构多智能体系统二分拟一致性

Bipartite quasi-consensus of heterogeneous multi-agent systems based on neural network approximation

控制与决策. 2023, 38(5): 1312-1318 https://doi.org/10.13195/j.kzyjc.2022.0611

带输出死区的多智能体系统预设时间事件触发式协同控制

Prescribed setting time event-triggered synergetic control of multiagent systems with output dead-zone

控制与决策. 2023, 38(2): 441-449 https://doi.org/10.13195/j.kzyjc.2021.0399

多智能体系统的事件触发无模型迭代学习双向一致性

Event-triggered model-free adaptive iterative learning bipartite consensus control for multi-agent systems

控制与决策. 2022, 37(10): 2552-2558 https://doi.org/10.13195/j.kzyjc.2021.0401

状态时延和全状态约束下的多智能体系统自适应事件触发控制

Adaptive event-triggered control for multi-agent systems with state time-delays and full state constraints

控制与决策. 2022, 37(4): 892-902 https://doi.org/10.13195/j.kzyjc.2020.1046

基于神经网络的周期扰动非线性系统自适应渐近跟踪控制

Neural-networks-based adaptive asymptotic tracking control for nonlinear systems with periodic disturbances

控制与决策. 2022, 37(4): 922-932 https://doi.org/10.13195/j.kzyjc.2020.1252

第38卷 第5期
2023年 5月

控 制 与 决 策
Control and Decision

Vol.38 No.5
May 2023

输出死区下的随机多智能体系统一致性饱和控制

于跃飞[1,3]，林国怀[1,3]，马 慧[2]，周 琪[1,3]，鲁仁全[1,3†]

(1. 广东工业大学 自动化学院，广州 510006；2. 广东工业大学 数学与统计学院，广州 510006；
3. 广东省智能决策与协同控制重点实验室，广州 510006)

摘　要: 针对一类存在输入饱和和输出死区现象的非严格反馈非线性随机多智能体系统,提出一种自适应神经网络一致性饱和控制算法. 首先,为了解决非对称输入饱和问题,构造一类与所考虑智能体相同阶次的辅助系统;然后,以反步法和辅助系统作为框架,利用神经网络处理系统中的未知非线性函数,并结合Nussbaum函数解决输出死区问题;接着,利用动态面控制技术避免“计算爆炸”问题;然后,基于李雅普诺夫稳定性理论验证所提出的控制算法能够保证闭环系统全部信号依概率半全局一致最终有界;最后,通过数值仿真和实例仿真的结果验证所提出控制算法的有效性.

关键词: 随机多智能体系统；一致性控制；输入饱和；输出死区

中图分类号: TP273　　　**文献标志码:** A

DOI: 10.13195/j.kzyjc.2022.0296　　　**开放科学(资源服务)标识码(OSID):**

引用格式: 于跃飞, 林国怀, 马慧, 等. 输出死区下的随机多智能体系统一致性饱和控制 [J]. 控制与决策, 2023, 38(5): 1249-1257.

Consensus saturation control for stochastic multi-agent systems with output dead zones

YU Yue-fei[1,3], *LIN Guo-huai*[1,3], *MA Hui*[2], *ZHOU Qi*[1,3], *LU Ren-quan*[1,3†]

(1. School of Automation，Guangdong University of Technology，Guangzhou 510006，China；2. School of Mathematics and Statistics，Guangdong University of Technology，Guangzhou 510006，China；3. Guangdong Province Key Laboratory of Intelligent Decision and Cooperative Control，Guangzhou 510006，China)

Abstract: An adaptive neural network consensus control algorithm is proposed for a class of non-strict feedback stochastic multi-agent systems with unknown input saturations and output dead zones. To solve the problem of asymmetric input saturations, an auxiliary system with the same order as the considered agent is constructed. Based on the framework of the backstepping method and the auxiliary system, neural networks are utilized to approximate the unknown nonlinear functions of multi-agent systems, and the Nussbaum function is introduced to compensate the negative effect of output dead zones. Moreover, the dynamic surface control technique is employed to avoid the problem of “explosion of complexity”. According to the Lyapunov stability theory, it is strictly proved that all signals in the closed-loop system are semi-globally uniformly ultimately bounded in probability. Finally, simulation results are provided to verify the effectiveness of the proposed control algorithm.

Keywords: stochastic multi-agent systems；consensus control；input saturations；output dead zones

0 引 言

多智能体系统的协同控制包括一致性控制[1-3]、包含控制[4-6]和编队控制[7-8]等,在人工智能和实际工程等领域[9-13]均有广泛的应用. 领导-跟随一致性控制作为多智能体系统协同控制的一种重要控制方式,其控制目标为通过智能体间的信息交互使得所有跟随者的状态趋向于领导者的状态. 针对多智能体系统的一致性跟踪控制问题,文献[1]考虑系统执行器遭遇突变故障和初始故障的情况,提出了一种新的分布式容错一致跟踪控制器. 文献[2]针对一类受到虚假数据注入攻击的多智能体系统,提出了一种新型事件触发一致性控制算法. 然而,许多实际系统不

收稿日期: 2022-02-25；**录用日期:** 2022-08-02.

基金项目: 国家自然科学基金项目(62121004, 62141606)；广东省研究生教育创新计划项目(2019JGXM40)；广东特支计划本土创新创业团队项目(2019BT02X353)；中国博士后科学基金项目(BX20220095, 2022M710826).

责任编委: 杨涛.

†通讯作者. E-mail: lurenquan2012@163.com.

仅仅是非线性的,且总是受到未知环境中各种随机扰动的影响. 随机扰动的存在会影响系统控制性能,甚至导致系统丧失稳定性,给系统是否可靠运行带来严峻的挑战. 针对存在随机扰动的多智能体系统一致性跟踪问题[14-17],文献[14]消除了关于随机系统的限制性假设,利用积分滑模面解决了不匹配不确定性问题. 文献[15]利用随机微分方程建模,并结合反步法技术提出了分布式自适应神经网络跟踪控制算法. 然而,在传统的反步法中,需要对虚拟控制器反复求导,即"计算爆炸"问题,导致计算量增加,使得控制器设计的过程复杂化. 文献[16-17]在不同约束条件下,结合反步法与动态面控制技术克服了此类问题. 由上述文献可知,尽管随机多智能体系统的一些控制问题得到了有效解决,但是当系统中同时出现输入饱和和输出死区现象时,如何利用反步法设计有效的控制器成为值得深入研究的问题.

在实际工程系统中不可避免地存在死区和约束等非线性非光滑现象,其中系统的死区现象包括输入死区和输出死区,而控制领域内的大多数研究集中于处理非线性系统中的输入死区问题[18-21]. 如文献[20]通过特定的模糊逻辑系统使得输入死区对系统的影响得到了有效抑制,并设计了一种自适应有限时间跟踪控制算法. 文献[21]建立了一种逻辑切换机制对不确定控制系数和输入死区进行补偿. 然而,上述结果均忽略了传感器可能出现死区现象. 事实上,输出死区会使得系统产生抖振甚至发生故障,导致系统控制输出失真和不稳定,从而严重影响多智能体系统的性能和信息交互过程. 文献[22-23]研究了系统在受到未知对称输出死区下的一致性跟踪控制问题. 文献[24]结合双曲正切函数的特性,提出了一种自适应模糊输出反馈控制算法. 以上文献虽然考虑了输出死区问题,但是没有考虑具有输出死区的随机多智能体系统饱和控制问题.

在实际系统运行过程中,当执行器输入达到极限值时,执行器输入的增加不会再影响输出,从而严重限制系统控制性能. 因此,如何设计有效的控制器保证具有输入饱和的系统实现稳定,引起了许多学者关注. 如文献[25-27]建立了输入饱和模型,将饱和函数近似为双曲正切函数,并设计饱和补偿系统对控制器信号进行补偿. 但是,当跟踪信号的幅值足够大时,这种方法可能会失效. 文献[28-29]通过引入辅助系统补偿执行器输入饱和,研究了一类具有输入饱和的随机非线性系统的稳定性和控制问题. 然而,上述控制方案无法直接应用于同时解决具有输入饱和和输出死区的随机多智能体系统控制问题.

基于以上讨论分析,本文研究一类具有输出死区的随机多智能体系统一致性饱和控制问题. 主要内容如下: 1) 与现有结果[25-27]相比,本文基于反步法的控制框架,设计与智能体相同阶次的辅助系统,产生多个辅助信号补偿非对称输入饱和的影响,揭示跟踪误差与输入饱和误差间的关系. 2) 本文考虑的多智能体系统受到输出死区影响,通过构造死区逆函数逼近死区模型并利用Nussbaum函数性质解决输出死区问题. 3) 在控制器设计过程中利用神经网络基函数的性质解决非严格反馈的"代数环"问题,并引入动态面控制技术有效避免"计算爆炸"问题,使得设计控制器的过程更简单.

1 预备知识与问题描述

假设系统中存在$N(N>0)$个智能体,定义多智能体间的有向图为$\psi=(\mathcal{H},\mathcal{E})$,其中:$\mathcal{H}=(1,2,\ldots,N)$,$\mathcal{E}\subseteq\mathcal{H}\times\mathcal{H}$为边集合. $(\mathcal{H}_j,\mathcal{H}_i)\in\mathcal{E}$表示智能体$j$的信息能够被智能体$i$接收,定义智能体$i$的邻居智能体集合为$\mathcal{N}_i=\{\mathcal{H}_j|(\mathcal{H}_j,\mathcal{H}_i)\in\mathcal{E},i\neq j\}$. 邻接矩阵$\mathcal{A}=[a_{i,j}]\in\boldsymbol{R}^{N\times N}$为智能体间的信息交互,$a_{i,j}>0$为智能体$i$可接受到智能体$j$的信息,否则$a_{i,j}=0$. 定义入度矩阵$\mathcal{M}=\mathrm{diag}\{m_1,m_2,\ldots,m_N\}$,其中$m_i=\sum\limits_{j\in\mathcal{N}_i}a_{i,j}$为智能体$i$的度,则$\mathcal{L}=\mathcal{M}-\mathcal{A}$为图$\psi$的拉普拉斯矩阵. 定义$\mathcal{G}=\mathrm{diag}\{a_{1,0},a_{2,0},\ldots,a_{N,0}\}$,当智能体$i$能够接收虚拟领导者0的信息时,$a_{i,0}>0$;否则$a_{i,0}=0$.

1.1 系统描述

本文考虑的随机多智能体系统由1个领导者和N个跟随者组成,其中第i个智能体的动态模型如下:

$$\begin{aligned}&\mathrm{d}x_{i,h}=(x_{i,h+1}+f_{i,h}(x_i))\mathrm{d}t+\phi_{i,h}^{\mathrm{T}}(x_i)\mathrm{d}\xi,\\&\mathrm{d}x_{i,n}=(u_i(v_i)+f_{i,n}(x_i))\mathrm{d}t+\phi_{i,n}^{\mathrm{T}}(x_i)\mathrm{d}\xi,\\&y_i=\varrho_i(x_{i,1}).\end{aligned}\tag{1}$$

其中:$h=1,2,\ldots,n-1;i=1,2,\ldots,N;x_i=[x_{i,1},x_{i,2},\ldots,x_{i,n}]^{\mathrm{T}}\in\boldsymbol{R}^n$为第$i$个智能体的状态向量;$f_{i,h}(x_i)$和$\phi_{i,h}(x_i)$为未知但光滑的非线性函数;$\xi$为在完全概率空间$(\varPhi,F,\{F_t\}_{t\geqslant0},P)$中的独立$r$维标准布朗运动;$u_i(v_i)$和$y_i$分别为第$i$个智能体的输入信号和输出信号. $u_i(v_i)$定义如下:

$$u_i(v_i)=\mathrm{sat}(v_i)=\begin{cases}u_{\max},\ v_i>u_{\max};\\v_i,\ u_{\min}\leqslant v_i\leqslant u_{\max};\\u_{\min},\ v_i<u_{\min}.\end{cases}$$

其中$u_{\max}$和$u_{\min}$为$u_i(v_i)$的未知上界和下界,$u_{\max}>0$且$u_{\min}<0$. 本文考虑的输出死区$\varrho_i(x_{i,1})$为非线性对

称死区,具有如下性质:

$$\varrho_i(x_{i,1})=\begin{cases}\varsigma_i(x_{i,1}-b_i),\ x_{i,1}>b_i;\\ 0,\ -b_i\leqslant x_{i,1}\leqslant b_i;\\ \varsigma_i(x_{i,1}+b_i),\ x_{i,1}<-b_i.\end{cases}\tag{2}$$

其中:死区斜率$\varsigma_i>0$,死区宽度$b_i>0$.

将式(2)改写为如下死区逆函数:

$$x_{i,1}=\varrho_i^{-1}(y_i)=\frac{1}{\varsigma_i}y_i+\frac{2b_i}{\pi_i}\arctan(k_iy_i),\tag{3}$$

其中k_i为大于0的调节参数. 式(3)可通过调节k_i逼近输出死区模型(2),有

$$\frac{\mathrm{d}x_{i,1}}{\mathrm{d}y_i}=\frac{1}{\varsigma_i}+\frac{2b_i}{\pi_i}\frac{k_i}{1+(k_iy_i)^2}.\tag{4}$$

由式(4)可得$0<\frac{1}{\varsigma_i}<\frac{\mathrm{d}x_{i,1}}{\mathrm{d}y_i},\dot{y}_i=\frac{(\mathrm{d}y_i/\mathrm{d}x_{i,1})}{\dot{x}_{i,1}}=\varsigma_i(t)\dot{x}_{i,1}$,其中$\varsigma_i(t)=\frac{\mathrm{d}y_i}{\mathrm{d}x_{i,1}}$,且$0<\varsigma_i(t)<\varsigma_i$.

本文引入了Nussbaum增益技术解决系统(1)中的输出死区问题,其中Nussbaum函数$N(\varpi)$具有如下性质:

$$\begin{cases}\lim\limits_{s\to\infty}\sup\frac{1}{s}\int_0^sN(\varpi)\mathrm{d}\varpi=+\infty,\\ \lim\limits_{s\to\infty}\inf\frac{1}{s}\int_0^sN(\varpi)\mathrm{d}\varpi=-\infty.\end{cases}$$

本文选择$N(\varpi_i)=\exp(\varpi_i^2)(\cos(\varpi_i^2)-\sin(\varpi_i^2))$.

引理1[17]　对于随机多智能体系统(1),定义$N(\varpi_i)$为Nussbaum函数,其中$\varpi_i(t)$在区间$[0,t_f)$上为光滑函数,且存在一个正定径向无界的函数$V(t,x)$满足如下不等式:

$$\ell V(t,x)\leqslant\\ -CV(t,x)+D+\sum_{i=1}^N(\varsigma_i(t)N(\varpi_i)+1)\dot{\varpi}_i.$$

其中:ℓ为微分算子,E为期望算子,$0<\varsigma_i(t)<\varsigma_i<\infty$,$C>0,D>0$. 则$E(V(t,x))$、$\varpi_i(t)$和$\sum_{i=1}^N(\varsigma_i(t)\times N(\varpi_i)+1)\dot{\varpi}_i$在区间$[0,t_f)$上是有界的.

1.2　随机系统

考虑如下随机非线性系统:

$$\mathrm{d}x=f(x)\mathrm{d}t+\phi(x)\mathrm{d}\xi.\tag{5}$$

其中:$x\in\boldsymbol{R}^n$为系统状态向量,ξ为r维标准布朗过程.

定义1[29]　考虑系统(5),假设存在连续可微的函数$V(x)\in C^2$,其微分算子ℓ可定义为

$$\ell V(x)=\frac{\partial V(x)}{\partial x}f(x)+\frac{1}{2}\mathrm{Tr}\Big\{\phi^{\mathrm{T}}(x)\frac{\partial^2V(x)}{\partial x^2}\phi(x)\Big\},$$

其中$\mathrm{Tr}\{\cdot\}$为矩阵的迹.

假设1[28]　随机多智能体系统(1)满足BIBS (bounded-input bounded-state stable)条件.

假设2[27]　虚拟领导者0的输出信号y_0为光滑函数,且y_0、$\dot{y}_0$和$\ddot{y}_0$均有界,即存在一个正数χ_0满足以下条件:$\Pi=\{(y_0,\dot{y}_0,\ddot{y}_0):y_0^2+\dot{y}_0^2+\ddot{y}_0^2\leqslant\chi_0\}$.

1.3　径向基神经网络

根据文献[16]和文献[23],对于多智能体系统中的未知连续非线性函数$f(\mathcal{Z})$,可利用径向基神经网络逼近$f(\mathcal{Z})$,具体表达式如下:

$$f(\mathcal{Z})=\omega^{*\mathrm{T}}\varphi(\mathcal{Z})+\delta(\mathcal{Z}),\ \forall\mathcal{Z}\in\Omega\subset\boldsymbol{R}^q.$$

其中:$\mathcal{Z}$为q维输入向量;$\delta(\mathcal{Z})$为逼近误差,且满足$|\delta(\mathcal{Z})|\leqslant\epsilon(\epsilon>0)$;$\varphi(\mathcal{Z})=[\varphi_1(\mathcal{Z}),\varphi_2(\mathcal{Z}),\dots,\varphi_k(\mathcal{Z})]^{\mathrm{T}}$为基函数向量,$\varphi_i(\mathcal{Z})$为高斯基函数,$k$为神经网络的节点数. 存在理想权重向量$\omega^*$使得以下方程成立:

$$\omega^*=\arg\min_{\omega\in\boldsymbol{R}^k}\{\sup_{\mathcal{Z}\in\Omega}|f(\mathcal{Z})-\omega^{\mathrm{T}}\varphi(\mathcal{Z})|\},$$

其中$\omega^*=[\omega_1^*,\omega_2^*,\dots,\omega_k^*]^{\mathrm{T}},\omega\in\boldsymbol{R}^k$为权重向量. 本文使用如下高斯基函数:

$$\varphi_i(\mathcal{Z})=\exp\Big(-\frac{(\mathcal{Z}-\iota_i)^{\mathrm{T}}(\mathcal{Z}-\iota_i)}{w_i^2}\Big).$$

其中:$i=1,2,\dots,k,\iota_i=[\iota_{i_1},\iota_{i_2},\dots,\iota_{i_q}]^{\mathrm{T}}$为中心向量,$w_i$为高斯基函数的宽度.

引理2[19]　对于状态向量$\bar{x}_j=[x_1,x_2,\dots,x_j]^{\mathrm{T}}$,其神经网络基函数向量为$\varphi(\bar{x}_j)=[\varphi_1(x_j),\varphi_2(x_j),\dots,\varphi_j(x_j)]^{\mathrm{T}}$,存在正整数$\rho(\rho\leqslant j)$,使得$\|\varphi(\bar{x}_j)\|^2\leqslant\|\varphi(\bar{x}_\rho)\|^2$.

引理3[23]　对于任意向量$x,y\in\boldsymbol{R}^n$,存在以下不等式成立:

$$x^{\mathrm{T}}y\leqslant\frac{p^a}{a}\|x\|^a+\frac{1}{bp^b}\|y\|^b.$$

其中:$p>0,a>1,b>1$,且$(a-1)(b-1)=1$.

2　神经网络控制器设计和稳定性分析

针对具有输入饱和和输出死区的随机多智能体系统(1),基于反步法和构造的辅助系统,本文设计了自适应神经网络控制器和参数自适应律,使得系统中所有信号均是依概率有界的.

为了处理系统中的输入饱和问题,构造如下辅助系统产生信号$l_{i,m}$:

$$\mathrm{d}l_{i,m}=(l_{i,m+1}-r_{i,m}l_{i,m})\mathrm{d}t.\tag{6}$$

其中:$i=1,2,\dots,N;m=1,2,\dots,n;l_{i,m}(0)=0$,$l_{i,n+1}=\Delta u_i,\Delta u_i=u_i(v_i)-v_i$为输入饱和误差;$r_{i,1},r_{i,2},\dots,r_{i,n}$均为大于0的设计参数.

注1　文献[25-27]直接使用光滑函数近似输入饱和函数,这种方法有一定的局限性,即跟踪误差依赖于参考信号y_0的振幅. 而本文设计的辅助系统(6)生成辅助信号$l_{i,m}$补偿输入饱和带来的负面影响.

第i个智能体的坐标变换设计如下:

$$s_{i,1}=\sum_{j\in\mathcal{N}_i}a_{i,j}(y_i-y_j)+a_{i,0}(y_i-y_0)-l_{i,1},$$

$$s_{i,h}=x_{i,h}-\lambda_{i,h}-l_{i,h},$$
$$z_{i,h}=\lambda_{i,h}-\alpha_{i,h-1},\ h=2,3,\ldots,n. \tag{7}$$

其中: $s_{i,1}$ 和 $s_{i,h}$ 为误差面, $z_{i,h}$ 为滤波误差, $\alpha_{i,h}$ 和 $\lambda_{i,h}$ 分别为虚拟控制信号和滤波器输出信号.

控制器设计的具体过程如下.

step 1: 根据式(1)、(6)和(7),可得

$$\mathrm{d}s_{i,1}=\Big(d_i\varsigma_i(t)(s_{i,2}+z_{i,2}+\alpha_{i,1}+f_{i,1}(x_i))-\sum_{j\in\mathcal{N}_i}a_{i,j}\varsigma_j(t)(x_{j,2}+f_{j,1}(x_j))+r_{i,1}l_{i,1}+(d_i\varsigma_i(t)-1)l_{i,2}-a_{i,0}\dot{y}_0\Big)\mathrm{d}t+\Big(d_i\varsigma_i(t)\times\phi_{i,1}^{\mathrm{T}}(x_i)-\sum_{j\in\mathcal{N}_i}a_{i,j}\varsigma_j(t)\phi_{j,1}^{\mathrm{T}}(x_j)\Big)\mathrm{d}\xi, \tag{8}$$

其中 $d_i=\sum_{j\in\mathcal{N}_i}a_{i,j}+a_{i,0}$. 选取李雅普诺夫函数为

$$V_{i,1}=\frac{1}{4}s_{i,1}^4+\frac{1}{2\eta_{i,1}}\tilde{\Theta}_{i,1}^2, \tag{9}$$

其中 $\eta_{i,1}>0$ 为设计参数. 定义 $\Theta_{i,m}^*=\|\omega_{i,m}^*\|^2, m=1,2,\ldots,n$. 令 $\hat{\Theta}_{i,m}$ 为 $\Theta_{i,m}^*$ 的估计, 且估计误差为 $\tilde{\Theta}_{i,m}=\Theta_{i,m}^*-\hat{\Theta}_{i,m}$.

结合定义1、式(8)和(9),可得

$$\ell V_{i,1}=\Big(d_i\varsigma_i(t)(s_{i,2}+z_{i,2}+\alpha_{i,1}+f_{i,1}(x_i))-\sum_{j\in\mathcal{N}_i}a_{i,j}\varsigma_j(t)(x_{j,2}+f_{j,1}(x_j))+r_{i,1}l_{i,1}+(d_i\varsigma_i(t)-1)l_{i,2}-a_{i,0}\dot{y}_0\Big)s_{i,1}^3-\frac{\tilde{\Theta}_{i,1}}{\eta_{i,1}}\dot{\hat{\Theta}}_{i,1}+\frac{3}{2}s_{i,1}^2\zeta_{i,1}^{\mathrm{T}}\zeta_{i,1}, \tag{10}$$

其中 $\zeta_{i,1}^{\mathrm{T}}=d_i\varsigma_i(t)\phi_{i,1}^{\mathrm{T}}(x_i)-\sum_{j\in\mathcal{N}_i}a_{i,j}\varsigma_j(t)\phi_{j,1}^{\mathrm{T}}(x_j)$.

由引理3,可得

$$s_{i,1}^3d_i\varsigma_i(t)s_{i,2}\leqslant\frac{3}{4}d_i^{\frac{4}{3}}\varsigma_i^{\frac{4}{3}}s_{i,1}^4+\frac{1}{4}s_{i,2}^4, \tag{11}$$

$$s_{i,1}^3d_i\varsigma_i(t)z_{i,2}\leqslant\frac{3}{4}d_i^{\frac{4}{3}}\varsigma_i^{\frac{4}{3}}s_{i,1}^4+\frac{1}{4}z_{i,2}^4, \tag{12}$$

$$\frac{3}{2}s_{i,1}^2\zeta_{i,1}^{\mathrm{T}}\zeta_{i,1}\leqslant\frac{3s_{i,1}^4}{4\kappa_{i,1}^2}\|\zeta_{i,1}\|^4+\frac{3}{4}\kappa_{i,1}^2, \tag{13}$$

其中 $\kappa_{i,1}>0$ 为设计参数.

将式(11)～(13)代入(10),可得

$$\ell V_{i,1}\leqslant\Big(d_i\varsigma_i(t)\alpha_{i,1}+\frac{3}{2}d_i^{\frac{4}{3}}\varsigma_i^{\frac{4}{3}}s_{i,1}+r_{i,1}l_{i,1}+\bar{f}_{i,1}\Big)s_{i,1}^3-\frac{\tilde{\Theta}_{i,1}}{\eta_{i,1}}\dot{\hat{\Theta}}_{i,1}+\frac{1}{4}(s_{i,2}^4+z_{i,2}^4)+\frac{3}{4}\kappa_{i,1}^2, \tag{14}$$

其中 $\bar{f}_{i,1}=d_i\varsigma_i(t)f_{i,1}(x_i)+(d_i\varsigma_i(t)-1)l_{i,2}+\sum_{j\in\mathcal{N}_i}a_{i,j}\varsigma_j(t)(x_{j,2}+f_{j,1}(x_j))+3s_{i,1}\|\zeta_{i,1}\|^4/(4\kappa_{i,1}^2)$.

利用神经网络逼近 $\bar{f}_{i,1}$,可得

$$\bar{f}_{i,1}=\omega_{i,1}^{*\mathrm{T}}\varphi_{i,1}(\underline{X}_{i,1})+\delta_{i,1}(\underline{X}_{i,1}).$$

其中: $\underline{X}_{i,1}=[l_{i,2},x_i^{\mathrm{T}},x_j^{\mathrm{T}}]^{\mathrm{T}}, j\in\mathcal{N}_i$; $\delta_{i,1}(\underline{X}_{i,1})$ 为逼近误差且 $|\delta_{i,1}(\underline{X}_{i,1})|\leqslant\epsilon_{i,1}$, $\epsilon_{i,1}$ 为大于0的常数.

由引理2和引理3,可得

$$s_{i,1}^3\bar{f}_{i,1}=s_{i,1}^3\left(\omega_{i,1}^{*\mathrm{T}}\varphi_{i,1}(\underline{X}_{i,1})+\delta_{i,1}(\underline{X}_{i,1})\right)\leqslant\frac{s_{i,1}^6}{2c_{i,1}^2}\Theta_{i,1}^*\varphi_{i,1}^{\mathrm{T}}(X_{i,1})\varphi_{i,1}(X_{i,1})+\frac{1}{2}c_{i,1}^2+\frac{3}{4}s_{i,1}^4+\frac{1}{4}\epsilon_{i,1}^4. \tag{15}$$

其中: $X_{i,1}=[x_{i,1},x_{j,1}]^{\mathrm{T}}, j\in\mathcal{N}_i$; $c_{i,1}>0$ 为设计参数.

设计虚拟控制信号 $\alpha_{i,1}$ 和参数自适应律 $\dot{\hat{\Theta}}_{i,1}$ 如下式所示:

$$\alpha_{i,1}=\frac{N(\varpi_i)}{d_i}\Big(\frac{s_{i,1}^3}{2c_{i,1}^2}\hat{\Theta}_{i,1}\varphi_{i,1}^{\mathrm{T}}(X_{i,1})\varphi_{i,1}(X_{i,1})+\Big(k_{i,1}+\frac{3}{2}d_i^{\frac{4}{3}}\varsigma_i^{\frac{4}{3}}+\frac{3}{4}\Big)s_{i,1}+r_{i,1}l_{i,1}-a_{i,0}\dot{y}_0\Big), \tag{16}$$

$$\dot{\hat{\Theta}}_{i,1}=\frac{\eta_{i,1}}{2c_{i,1}^2}s_{i,1}^6\varphi_{i,1}^{\mathrm{T}}(X_{i,1})\varphi_{i,1}(X_{i,1})-\sigma_{i,1}\hat{\Theta}_{i,1}, \tag{17}$$

$$\dot{\varpi}_i=s_{i,1}^3\Big(\Big(k_{i,1}+\frac{3}{2}d_i^{\frac{4}{3}}\varsigma_i^{\frac{4}{3}}+\frac{3}{4}\Big)s_{i,1}+r_{i,1}l_{i,1}+\frac{s_{i,1}^3}{2c_{i,1}^2}\hat{\Theta}_{i,1}\varphi_{i,1}^{\mathrm{T}}(X_{i,1})\varphi_{i,1}(X_{i,1})-a_{i,0}\dot{y}_0\Big), \tag{18}$$

其中 $k_{i,1}>0$ 和 $\sigma_{i,1}>0$ 为设计参数.

将式(15)～(18)代入(14),可得

$$\ell V_{i,1}\leqslant(\varsigma_i(t)N(\varpi_i)+1)\dot{\varpi}_i-k_{i,1}s_{i,1}^4+\frac{\sigma_{i,1}}{\eta_{i,1}}\times\tilde{\Theta}_{i,1}\hat{\Theta}_{i,1}+\frac{1}{2}\Big(c_{i,1}^2+\frac{3}{2}\kappa_{i,1}^2+\frac{1}{2}\epsilon_{i,1}^4\Big)+\frac{1}{4}(s_{i,2}^4+z_{i,2}^4). \tag{19}$$

step 2: 为了避免对 $\alpha_{i,h-1}(2\leqslant h\leqslant n-1)$ 反复偏微分,令 $\alpha_{i,h-1}$ 通过一阶滤波器得到 $\lambda_{i,h}$,则

$$\tau_{i,h}\dot{\lambda}_{i,h}+\lambda_{i,h}=\alpha_{i,h-1}.$$

其中: $\lambda_{i,h}(0)=\alpha_{i,h-1}(0)$, $\tau_{i,h}>0$ 为时间常数.

由式(1)、(6)和(7),结合定义1可得

$$\mathrm{d}s_{i,h}=(s_{i,h+1}+z_{i,h+1}+\alpha_{i,h}+f_{i,h}(x_i)+r_{i,h}l_{i,h}-\dot{\lambda}_{i,h})\mathrm{d}t+\phi_{i,h}^{\mathrm{T}}(x_i)\mathrm{d}\xi,$$
$$\mathrm{d}z_{i,h}=\Big(-\frac{z_{i,h}}{\tau_{i,h}}+B_{i,h}\Big)\mathrm{d}t+I_{i,h}\mathrm{d}\xi. \tag{20}$$

注2 根据文献[16]和文献[17], $B_{i,h}$ 和 $I_{i,h}$ 为对式(16)中的 $\alpha_{i,1}$ 求偏导得到的,故存在大于0的常数 $\bar{B}_{i,h}$ 和 $\bar{I}_{i,h}$,满足 $|B_{i,h}|\leqslant\bar{B}_{i,h}$, $\mathrm{Tr}\{I_{i,h}^{\mathrm{T}}I_{i,h}\}\leqslant\bar{I}_{i,h}$.

选取第 h 步的李雅普诺夫函数为

$$V_{i,h}=V_{i,h-1}+\frac{1}{4}s_{i,h}^4+\frac{1}{4}z_{i,h}^4+\frac{1}{2\eta_{i,h}}\tilde{\Theta}_{i,h}^2, \tag{21}$$

其中 $\eta_{i,h}>0$ 为设计参数.

由定义1、式(20)和(21),可得

$$\ell V_{i,h}=\ell V_{i,h-1}+s_{i,h}^3(s_{i,h+1}+z_{i,h+1}+\alpha_{i,h}+f_{i,h}(x_i)+r_{i,h}l_{i,h}-\dot{\lambda}_{i,h})-\frac{\tilde{\Theta}_{i,h}}{\eta_{i,h}}\dot{\hat{\Theta}}_{i,h}+\frac{3}{2}z_{i,h}^2\mathrm{Tr}\{I_{i,h}^{\mathrm{T}}I_{i,h}\}+\frac{3}{2}s_{i,h}^2\phi_{i,h}^{\mathrm{T}}(x_i)\times\phi_{i,h}(x_i)+z_{i,h}^3\Big(-\frac{z_{i,h}}{\tau_{i,h}}+B_{i,h}\Big).\tag{22}$$

由引理3, 可得

$$s_{i,h}^3s_{i,h+1}\leqslant\frac{3}{4}s_{i,h}^4+\frac{1}{4}s_{i,h+1}^4,\tag{23}$$

$$s_{i,h}^3z_{i,h+1}\leqslant\frac{3}{4}s_{i,h}^4+\frac{1}{4}z_{i,h+1}^4,\tag{24}$$

$$z_{i,h}^3B_{i,h}\leqslant\frac{3}{4}z_{i,h}^4+\frac{1}{4}\bar{B}_{i,h}^4,\tag{25}$$

$$\frac{3}{2}z_{i,h}^2\mathrm{Tr}\{I_{i,h}^{\mathrm{T}}I_{i,h}\}\leqslant\frac{3\bar{I}_{i,h}^2}{4\mu_{i,h}^2}z_{i,h}^4+\frac{3}{4}\mu_{i,h}^2,\tag{26}$$

$$\frac{3}{2}s_{i,h}^2\phi_{i,h}^{\mathrm{T}}(x_i)\phi_{i,h}(x_i)\leqslant\frac{3s_{i,h}^4}{4\kappa_{i,h}^2}\|\phi_{i,h}(x_i)\|^4+\frac{3}{4}\kappa_{i,h}^2,\tag{27}$$

其中$\kappa_{i,h}>0$和$\mu_{i,h}>0$为设计参数.

将式(23)~(27)代入(22), 可得

$$\ell V_{i,h}\leqslant\ell V_{i,h-1}-\frac{1}{4}(s_{i,h}^4+z_{i,h}^4)+\frac{1}{4}\bar{B}_{i,h}^4+s_{i,h}^3\times\Big(\alpha_{i,h}+\frac{7}{4}s_{i,h}+\bar{f}_{i,h}+r_{i,h}l_{i,h}-\dot{\lambda}_{i,h}\Big)-z_{i,h}^4\Big(\frac{1}{\tau_{i,h}}-\frac{3\bar{I}_{i,h}^2}{4\mu_{i,h}^2}-1\Big)-\frac{\tilde{\Theta}_{i,h}}{\eta_{i,h}}\dot{\hat{\Theta}}_{i,h}+\frac{1}{4}(s_{i,h+1}^4+z_{i,h+1}^4)+\frac{3}{4}\kappa_{i,h}^2+\frac{3}{4}\mu_{i,h}^2,\tag{28}$$

其中$\bar{f}_{i,h}=f_{i,h}(x_i)+3s_{i,h}\|\phi_{i,h}(x_i)\|^4/(4\kappa_{i,h}^2)$.

类似于式(15), 可得

$$s_{i,h}^3\bar{f}_{i,h}\leqslant\frac{s_{i,h}^6}{2c_{i,h}^2}\Theta_{i,h}^*\varphi_{i,h}^{\mathrm{T}}(X_{i,h})\varphi_{i,h}(X_{i,h})+\frac{1}{2}c_{i,h}^2+\frac{3}{4}s_{i,h}^4+\frac{1}{4}\epsilon_{i,h}^4.\tag{29}$$

其中: $X_{i,h}=[x_{i,1},x_{i,2},\dots,x_{i,h}]^{\mathrm{T}}$, $c_{i,h}>0$为设计参数.

设计第h步的虚拟控制信号$\alpha_{i,h}$和参数自适应律$\dot{\hat{\Theta}}_{i,h}$如下式所示:

$$\alpha_{i,h}=-\Big(k_{i,h}+\frac{5}{2}\Big)s_{i,h}-r_{i,h}l_{i,h}+\dot{\lambda}_{i,h}-\frac{s_{i,h}^3}{2c_{i,h}^2}\hat{\Theta}_{i,h}\varphi_{i,h}^{\mathrm{T}}(X_{i,h})\varphi_{i,h}(X_{i,h}),\tag{30}$$

$$\dot{\hat{\Theta}}_{i,h}=\frac{\eta_{i,h}}{2c_{i,h}^2}s_{i,h}^6\varphi_{i,h}^{\mathrm{T}}(X_{i,h})\varphi_{i,h}(X_{i,h})-\sigma_{i,h}\hat{\Theta}_{i,h},\tag{31}$$

其中$k_{i,h}>0$和$\sigma_{i,h}>0$为设计参数.

将式(29)~(31)代入(28), 可得

$$\ell V_{i,h}\leqslant\ell V_{i,h-1}-\frac{1}{4}(s_{i,h}^4+z_{i,h}^4)-k_{i,h}s_{i,h}^4-\Big(\frac{1}{\tau_{i,h}}-\frac{3\bar{I}_{i,h}^2}{4\mu_{i,h}^2}-1\Big)z_{i,h}^4+\frac{\sigma_{i,h}}{\eta_{i,h}}\tilde{\Theta}_{i,h}\hat{\Theta}_{i,h}+\frac{1}{4}(s_{i,h+1}^4+z_{i,h+1}^4)+\frac{1}{4}(3\mu_{i,h}^2+\bar{B}_{i,h}^4)+\frac{1}{2}\Big(c_{i,h}^2+\frac{3}{2}\kappa_{i,h}^2+\frac{1}{2}\epsilon_{i,h}^4\Big).\tag{32}$$

step 3: 选取第n步李雅普诺夫函数为

$$V_{i,n}=V_{i,n-1}+\frac{1}{4}s_{i,n}^4+\frac{1}{4}z_{i,n}^4+\frac{1}{2\eta_{i,n}}\tilde{\Theta}_{i,n}^2,\tag{33}$$

其中$\eta_{i,n}>0$为设计参数. 结合定义1和式(33), 可得

$$\ell V_{i,n}=\ell V_{i,n-1}+s_{i,n}^3(v_i+f_{i,n}(x_i)+r_{i,n}l_{i,n}-\dot{\lambda}_{i,n})+\frac{3}{2}s_{i,n}^2\phi_{i,n}^{\mathrm{T}}(x_i)\phi_{i,n}(x_i)+z_{i,n}^3\times\Big(-\frac{z_{i,n}}{\tau_{i,n}}+B_{i,n}\Big)-\frac{1}{\eta_{i,n}}\tilde{\Theta}_{i,n}\dot{\hat{\Theta}}_{i,n}+\frac{3}{2}z_{i,n}^2\mathrm{Tr}\{I_{i,n}^{\mathrm{T}}I_{i,n}\}.\tag{34}$$

由引理3, 式(34)中的$z_{i,n}^3B_{i,n}$、$\frac{3}{2}z_{i,n}^2\mathrm{Tr}\{I_{i,n}^{\mathrm{T}}I_{i,n}\}$和$\frac{3}{2}s_{i,n}^2\phi_{i,n}^{\mathrm{T}}(x_i)\phi_{i,n}(x_i)$可类似于式(25)~(27)进行放缩, 得到

$$\ell V_{i,n}\leqslant\ell V_{i,n-1}-\frac{1}{4}(s_{i,n}^4+z_{i,n}^4)+s_{i,n}^3\Big(v_i+\bar{f}_{i,n}+\frac{1}{4}s_{i,n}+r_{i,n}l_{i,n}-\dot{\lambda}_{i,n}\Big)-z_{i,n}^4\times\Big(\frac{1}{\tau_{i,n}}-\frac{3\bar{I}_{i,n}^2}{4\mu_{i,n}^2}-1\Big)-\frac{\tilde{\Theta}_{i,n}}{\eta_{i,n}}\dot{\hat{\Theta}}_{i,n}+\frac{3}{4}\kappa_{i,n}^2+\frac{1}{4}(3\mu_{i,n}^2+\bar{B}_{i,n}^4).\tag{35}$$

其中: $\mu_{i,n}>0$和$\kappa_{i,n}>0$为设计参数; 且$|B_{i,n}|\leqslant\bar{B}_{i,n}$, $\mathrm{Tr}\{I_{i,n}^{\mathrm{T}}I_{i,n}\}\leqslant\bar{I}_{i,n}$, $\bar{B}_{i,n}$和$\bar{I}_{i,n}$为大于0的常数; $\bar{f}_{i,n}=f_{i,n}(x_i)+3s_{i,n}\|\phi_{i,n}(x_i)\|^4/(4\kappa_{i,n}^2)$.

由引理3, 可得

$$s_{i,n}^3\bar{f}_{i,n}\leqslant\frac{s_{i,n}^6}{2c_{i,n}^2}\Theta_{i,n}^*\varphi_{i,n}^{\mathrm{T}}(X_{i,n})\varphi_{i,n}(X_{i,n})+\frac{1}{2}c_{i,n}^2+\frac{3}{4}s_{i,n}^4+\frac{1}{4}\epsilon_{i,n}^4,\tag{36}$$

其中$c_{i,n}>0$为设计参数.

控制器v_i和参数自适应律$\dot{\hat{\Theta}}_{i,n}$设计如下:

$$v_i=-(k_{i,n}+1)s_{i,n}-r_{i,n}l_{i,n}+\dot{\lambda}_{i,n}-\frac{s_{i,n}^3}{2c_{i,n}^2}\hat{\Theta}_{i,n}\varphi_{i,n}^{\mathrm{T}}(X_{i,n})\varphi_{i,n}(X_{i,n}),\tag{37}$$

$$\dot{\hat{\Theta}}_{i,n}=\frac{\eta_{i,n}}{2c_{i,n}^2}s_{i,n}^6\varphi_{i,n}^{\mathrm{T}}(X_{i,n})\varphi_{i,n}(X_{i,n})-\sigma_{i,n}\hat{\Theta}_{i,n},\tag{38}$$

其中$k_{i,n}>0$和$\sigma_{i,n}>0$为设计参数.

将式(36)~(38)代入(35), 可得

$$\ell V_{i,n}\leqslant\ell V_{i,n-1}-\frac{1}{4}(s_{i,n}^4+z_{i,n}^4)-k_{i,n}s_{i,n}^4-$$

$$\Big(\frac{1}{\tau_{i,n}}-\frac{3\bar{I}_{i,n}^2}{4\mu_{i,n}^2}-1\Big)z_{i,n}^4+\frac{\sigma_{i,n}}{\eta_{i,n}}\tilde{\Theta}_{i,n}\times$$
$$\hat{\Theta}_{i,n}+\frac{1}{2}\Big(c_{i,n}^2+\frac{3}{2}\kappa_{i,n}^2+\frac{1}{2}\epsilon_{i,n}^4\Big)+$$
$$\frac{1}{4}(3\mu_{i,n}^2+\bar{B}_{i,n}^4). \tag{39}$$

根据上述结果,可类推出$\ell V_{i,n-1}$为

$$\ell V_{i,n-1}\leqslant(\varsigma_i(t)N(\varpi_i)+1)\dot{\varpi}_i-\sum_{j=1}^{n-1}k_{i,j}s_{i,j}^4-$$
$$\sum_{j=2}^{n-1}\Big(\frac{1}{\tau_{i,j}}-\frac{3\bar{I}_{i,j}^2}{4\mu_{i,j}^2}-1\Big)z_{i,j}^4+\sum_{j=1}^{n-1}\frac{\sigma_{i,j}}{\eta_{i,j}}\times$$
$$\tilde{\Theta}_{i,j}\hat{\Theta}_{i,j}+\frac{1}{2}\sum_{j=1}^{n-1}\Big(c_{i,j}^2+\frac{3}{2}\kappa_{i,j}^2+\frac{1}{2}\epsilon_{i,j}^4\Big)+$$
$$\frac{1}{4}\sum_{j=2}^{n-1}(3\mu_{i,j}^2+\bar{B}_{i,j}^4)+\frac{1}{4}(s_{i,n}^4+z_{i,n}^4). \tag{40}$$

将式(40)代入(39),可得

$$\ell V_{i,n}\leqslant(\varsigma_i(t)N(\varpi_i)+1)\dot{\varpi}_i-\sum_{j=1}^{n}k_{i,j}s_{i,j}^4-$$
$$\sum_{j=2}^{n}\Big(\frac{1}{\tau_{i,j}}-\frac{3\bar{I}_{i,j}^2}{4\mu_{i,j}^2}-1\Big)z_{i,j}^4+\sum_{j=1}^{n}\frac{\sigma_{i,j}}{\eta_{i,j}}\times$$
$$\tilde{\Theta}_{i,j}\hat{\Theta}_{i,j}+\frac{1}{2}\sum_{j=1}^{n}\Big(c_{i,j}^2+\frac{3}{2}\kappa_{i,j}^2+\frac{1}{2}\epsilon_{i,j}^4\Big)+$$
$$\frac{1}{4}\sum_{j=2}^{n}(3\mu_{i,j}^2+\bar{B}_{i,j}^4). \tag{41}$$

由引理3,可得

$$\frac{\sigma_{i,j}}{\eta_{i,j}}\tilde{\Theta}_{i,j}\hat{\Theta}_{i,j}\leqslant-\frac{\sigma_{i,j}}{2\eta_{i,j}}\tilde{\Theta}_{i,j}^2+\frac{\sigma_{i,j}}{2\eta_{i,j}}\Theta_{i,j}^{*2}. \tag{42}$$

将式(42)代入(41),可得

$$\ell V_{i,n}\leqslant\big(\varsigma_i(t)N(\varpi_i)+1\big)\dot{\varpi}_i-\sum_{j=1}^{n}k_{i,j}s_{i,j}^4-$$
$$\sum_{j=2}^{n}\bar{\tau}_{i,j}z_{i,j}^4-\sum_{j=1}^{n}\frac{\sigma_{i,j}}{2\eta_{i,j}}\tilde{\Theta}_{i,j}^2+D_i. \tag{43}$$

其中

$$\bar{\tau}_{i,j}=\frac{1}{\tau_{i,j}}-\frac{3\bar{I}_{i,j}^2}{4\mu_{i,j}^2}-1,$$
$$D_i=\sum_{j=1}^{n}\frac{\sigma_{i,j}}{2\eta_{i,j}}\Theta_{i,j}^{*2}+\frac{1}{4}\sum_{j=2}^{n}(3\mu_{i,j}^2+\bar{B}_{i,j}^4)+$$
$$\frac{1}{2}\sum_{j=1}^{n}\Big(c_{i,j}^2+\frac{3}{2}\kappa_{i,j}^2+\frac{1}{2}\epsilon_{i,j}^4\Big).$$

定义$C_i=\min\limits_{j=2,3,\dots,n}\{4k_{i,1},4k_{i,j},\sigma_{i,1},\sigma_{i,j},4\bar{\tau}_{i,j}\}$,式(43)可改写为

$$\ell V_{i,n}\leqslant-C_iV_{i,n}+(\varsigma_i(t)N(\varpi_i)+1)\dot{\varpi}_i+D_i. \tag{44}$$

选取李雅普诺夫函数

$$V=\sum_{i=1}^{N}V_{i,n}, \tag{45}$$

由式(44)和(45),则

$$\ell V\leqslant-CV+\sum_{i=1}^{N}(\varsigma_i(t)N(\varpi_i)+1)\dot{\varpi}_i+\bar{D}. \tag{46}$$

其中: $C=\min\limits_{1\leqslant i\leqslant N}\{C_i\},\bar{D}=\sum\limits_{i=1}^{N}D_i$. 根据引理1可得, $\sum\limits_{i=1}^{N}(\varsigma_i(t)N(\varpi_i)+1)\dot{\varpi}_i$在区间$[0,t_f)$上有界,则式(46)可改写为

$$\ell V\leqslant-CV+D, \tag{47}$$

其中$D=\max\limits_{t\in[0,t_f)}\sum\limits_{i=1}^{N}(\varsigma_i(t)N(\varpi_i)+1)\dot{\varpi}_i+\bar{D}$. 由式(9)和(47),可得

$$E\Big(\sum_{i=1}^{N}|s_{i,1}(t)|^4\Big)\leqslant4\Big(\mathrm{e}^{-Ct}V(0)+\frac{D}{C}\Big). \tag{48}$$

令$e_i=\sum\limits_{j\in N_i}a_{i,j}(y_i-y_j)+a_{i,0}(y_i-y_0)$, e_i为系统(1)的一致性误差,并根据不等式$|e_i|^4\leqslant8|l_{i,1}|^4+8|s_{i,1}(t)|^4$,可得

$$E\Big(\sum_{i=1}^{N}|e_i|^4\Big)\leqslant$$
$$8\Big(E\Big(\sum_{i=1}^{N}|l_{i,1}|^4\Big)+E\Big(\sum_{i=1}^{N}|s_{i,1}(t)|^4\Big)\Big). \tag{49}$$

为了证明$E\Big(\sum\limits_{i=1}^{N}|l_{i,1}|^4\Big)$有界,选择李雅普诺夫函数为$V_l=\frac{1}{4}\sum\limits_{i=1}^{N}\sum\limits_{m=1}^{n}l_{i,m}^4$. 由式(6),可得

$$\ell V_l\leqslant-\sum_{i=1}^{N}\sum_{m=1}^{n}\bar{r}_{i,m}l_{i,m}^4+\frac{1}{4}\sum_{i=1}^{N}(\Delta u_i)^4\leqslant$$
$$-RV_l+\tilde{D}. \tag{50}$$

其中: $\bar{r}_{i,1}=r_{i,1}-\frac{3}{4},\bar{r}_{i,\sigma}=r_{i,\sigma}-1,\sigma=2,3,\dots,n,R=4\min\limits_{1\leqslant i\leqslant N}(\bar{r}_{i,1},\bar{r}_{i,2},\dots,\bar{r}_{i,n}),\tilde{D}=\frac{1}{4}\sum\limits_{i=1}^{N}(\Delta u_i)^4$. 由式(50),可得

$$E(V_l(t))\leqslant\mathrm{e}^{-Rt}V_l(0)+\frac{1}{R}\sup_{0\leqslant s\leqslant t}\tilde{D}. \tag{51}$$

其中: $V_l(0)=0,l_{i,m}(0)=0$, s为$[0,t]$上的某一时刻. 则由假设1和式(51),可得$E\Big(\sum\limits_{i=1}^{N}|l_{i,1}|^4\Big)$有界,即

$$E\Big(\sum_{i=1}^{N}|l_{i,1}|^4\Big)\leqslant\frac{4}{R}\sup_{0\leqslant s\leqslant t}\tilde{D}. \tag{52}$$

由式(49)和(52),可得

$$\lim_{t\to\infty} E\Big(\sum_{i=1}^{N}|e_i|^4\Big) \leqslant 32\Big(\frac{D}{C}+\frac{1}{R}\sup_{s\geqslant 0}\tilde{D}\Big). \tag{53}$$

由式(53)可知,通过选择合适的设计参数,可使得一致性误差e_i收敛至原点附近的邻域内.

根据上述设计方案和分析,可得到以下定理.

定理1　对于含有输入饱和和输出死区的非严格反馈随机多智能体系统(1),在假设1和假设2成立的前提下,通过设计辅助系统(6)、坐标变换(7)、虚拟控制信号(16)和(30)、控制器(37)以及参数自适应律(17)、(31)和(38),可保证闭环系统的全部信号均是依概率有界的,且一致性误差e_i收敛至原点附近的邻域内.

3　仿真实验

在本节中,通过2个仿真例子验证该算法的有效性. 图1为仿真的通信拓扑图,随机多智能体系统由1个虚拟领导者和4个跟随者组成,分别标记为0、1、2、3、4.

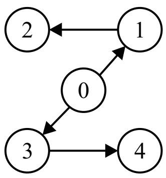

图1　通信拓扑

数值仿真　考虑如下二阶随机多智能体系统:

$$\begin{aligned}&\mathrm{d}x_{i,1}=(x_{i,2}+f_{i,1}(x_i))\mathrm{d}t+\phi_{i,1}(x_i)\mathrm{d}\xi,\\&\mathrm{d}x_{i,2}=(u_i(v_i)+f_{i,2}(x_i))\mathrm{d}t+\phi_{i,2}(x_i)\mathrm{d}\xi,\\&y_i=\varrho_i(x_{i,1}),\ i=1,2,3,4.\end{aligned}$$

其中: $f_{i,1}(x_i)=0.5x_{i,1}^2x_{i,2}, f_{i,2}(x_i)=-0.25(x_{i,1}+x_{i,2}), \phi_{i,1}(x_i)=x_{i,2}+\sin(x_{i,1}), \phi_{i,2}(x_i)=2\sin(x_{i,1}x_{i,2})$.

假设领导者的输出信号$y_0=1.5\sin(0.5t)$,选择适当的设计参数为$k_{1,1}=k_{3,1}=40, k_{2,1}=k_{4,1}=60, k_{i,2}=20, \eta_{i,1}=\eta_{i,2}=c_{i,1}=c_{i,2}=\sigma_{i,1}=\sigma_{i,2}=1, \tau_{i,1}=0.05, r_{i,1}=20, r_{i,2}=5, u_{\max}=3, u_{\min}=-3, b_i=0.04, \varsigma_i=1$. 初始值设置为$x_{1,1}(0)=0.035, x_{2,1}(0)=0.015, x_{3,1}(0)=0.04, x_{4,1}(0)=0.02, x_{1,2}(0)=0.15, x_{2,2}(0)=0.05, x_{3,2}(0)=0.2, x_{4,2}(0)=0.08, \hat{\Theta}_{1,1}(0)=0.5, \hat{\Theta}_{2,1}(0)=0.35, \hat{\Theta}_{3,1}(0)=0.2, \hat{\Theta}_{4,1}(0)=0.6, \hat{\Theta}_{1,2}(0)=0.15, \hat{\Theta}_{2,2}(0)=0.25, \hat{\Theta}_{3,2}(0)=0.16, \hat{\Theta}_{4,2}(0)=0.23, l_{i,1}(0)=l_{i,2}(0)=0, \varpi_i(0)=1.28, i=1,2,3,4$.

图2～图4为数值仿真的结果. 图2为在所提出控制算法下的领导者参考信号y_0和跟随者输出信号y_i的响应曲线. 图3为3种控制算法下以第1个智能体为例的跟踪效果对比,其中: AS为基于辅助系统的控制算法, AF为基于函数逼近技术的控制算法. 图4为控制信号$u_i(v_i)$的轨迹, $u_i(v_i)$始终在$[u_{\min}, u_{\max}]$内. 由图2～图4可见,所设计控制算法能够解决系统中的输入饱和问题,并使得跟随者的输出信号能够较好地跟踪上参考信号.

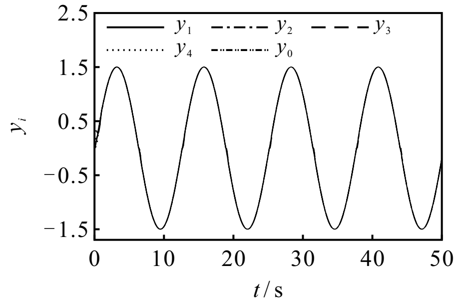

图2　参考信号y_0和输出信号y_i

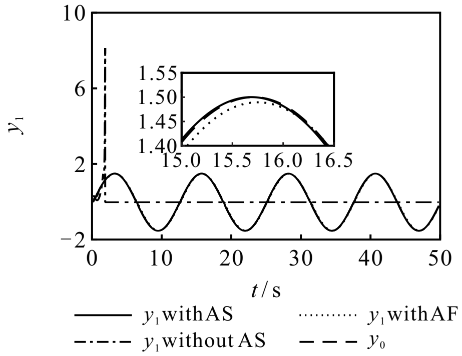

图3　不同控制算法下的智能体输出信号y_1

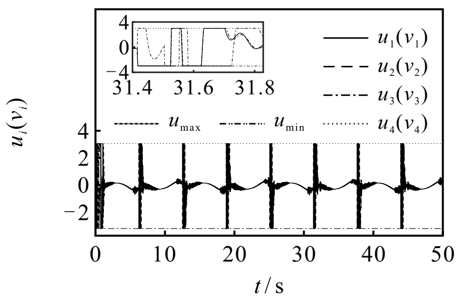

图4　控制信号

实例仿真　考虑单连杆多机械臂系统,其动力学方程为

$$J_i\ddot{\gamma}_i=-M_igl_i\sin\gamma_i-B_i\dot{\gamma}_i+u_i(v_i). \tag{54}$$

其中: J_i为电机的总转动惯量, M_i和l_i为连杆的质量和长度, $B_i\dot{\gamma}_i$为具有阻尼系数B_i的粘性阻尼. 令$x_{i,1}=\gamma_i, x_{i,2}=\dot{\gamma}_i$,式(54)可改写为

$$\begin{aligned}&\mathrm{d}x_{i,1}=x_{i,2}\mathrm{d}t+\phi_{i,1}(x_i)\mathrm{d}\xi,\\&\mathrm{d}x_{i,2}=\Big(\frac{u_i(v_i)}{J_i}+f_{i,2}(x_i)\Big)\mathrm{d}t+\phi_{i,2}(x_i)\mathrm{d}\xi,\\&y_i=\varrho_i(x_{i,1}),\ i=1,2,3,4.\end{aligned}$$

其中: $\phi_{i,1}(x_i)=\phi_{i,2}(x_i)=0.5(x_{i,1}+x_{i,2}), f_{i,2}(x_i)=-M_ig\sin(x_{i,1})/(J_il_i)-B_ix_{i,2}/J_i$.

假设虚拟领导者的输出信号为$y_0=0.8\sin(t)$. 取$M_i=0.5\,\mathrm{kg}, J_i=1\,\mathrm{kg\cdot m^2}, g=9.8\,\mathrm{m/s^2}, l_i=0.8\,\mathrm{m}, B_i=0.5\,\mathrm{N\cdot m\cdot s}$. 选择适当的设计参数为$k_{1,1}=k_{3,1}=50, k_{2,1}=k_{4,1}=100, k_{i,2}=20, \eta_{i,1}=\eta_{i,2}=c_{i,1}=c_{i,2}=\sigma_{i,1}=\sigma_{i,2}=1, \tau_{i,1}=0.05, r_{i,1}=50, r_{i,2}=5, u_{\max}=7, u_{\min}=-9, b_i=0.04, \varsigma_i=1$. 初始值设置为$x_{1,1}(0)=0.2, x_{2,1}(0)=0.05, x_{3,1}(0)=0.1, x_{4,1}(0)=0.15, x_{1,2}(0)=0.25, x_{2,2}(0)=0.15, x_{3,2}(0)=0.1, x_{4,2}(0)=0.3, \hat{\Theta}_{1,1}(0)=0.3, \hat{\Theta}_{2,1}(0)=0.6, \hat{\Theta}_{3,1}(0)=0.2, \hat{\Theta}_{4,1}(0)=0.5, \hat{\Theta}_{1,2}(0)=0.4, \hat{\Theta}_{2,2}(0)=0.15, \hat{\Theta}_{3,2}(0)=0.3, \hat{\Theta}_{4,2}(0)=0.5, l_{i,1}(0)=l_{i,2}(0)=0, \varpi_i(0)=1.28, i=1,2,3,4$.

图5和图6为实例仿真的结果. 图5为参考信号y_0和跟随者输出信号y_i的响应曲线. 图6为控制信号$u_i(v_i)$的轨迹, 由图6可见, 控制信号$u_i(v_i)$始终保持在$u_{\max}=7$和$u_{\min}=-9$的约束范围内.

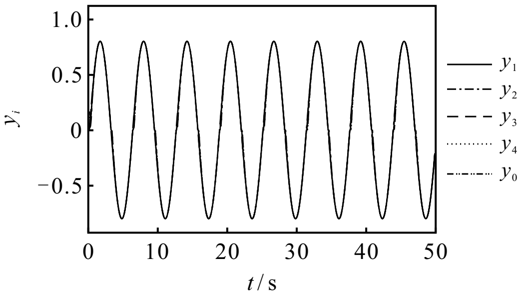

图5 参考信号y_0和输出信号y_i

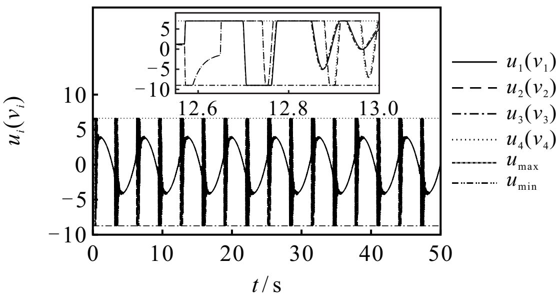

图6 控制信号

由数值仿真和实例仿真可见, 在随机多智能体系统和随机多机械臂系统受到输入饱和和输出死区影响的情况下, 所提出自适应神经网络一致性控制算法仍然能够保证系统实现稳定, 并能够获得较好的跟踪效果.

4 结论

本文研究了一类具有输入饱和和输出死区的随机多智能体系统一致性跟踪问题, 提出了一种有效的自适应神经网络一致性控制算法. 在控制算法设计过程中, 通过辅助系统产生的多个信号补偿输入饱和的影响, 结合Nussbaum函数性质解决输出死区问题. 基于李雅普诺夫稳定性理论验证了闭环系统中全部信号均是依概率有界的. 最后, 通过数值仿真和实例仿真验证了该控制算法的有效性. 在今后的研究中, 将把本文的结果推广到状态未知或状态受约束的非线性随机多智能体系统中.

参考文献(References)

[1] Liu C, Jiang B, Zhang K, et al. Distributed fault-tolerant consensus tracking control of multi-agent systems under fixed and switching topologies[J]. IEEE Transactions on Circuits and Systems I: Regular Papers, 2021, 68(4): 1646-1658.

[2] Li X M, Zhou Q, Li P S, et al. Event-triggered consensus control for multi-agent systems against false data-injection attacks[J]. IEEE Transactions on Cybernetics, 2020, 50(5): 1856-1866.

[3] 周托, 刘全利, 王东, 等. 积分事件触发策略下的线性多智能体系统领导跟随一致性[J]. 控制与决策, 2022, 37(5): 1258-1266.
(Zhou T, Liu Q L, Wang D, et al. Leader-following consensus for linear multi-agent systems based on integral-type event-triggered strategy[J]. Control and Decision, 2022, 37(5): 1258-1266.)

[4] Wang L X, Liu X Y, Cao J D, et al. Fixed-time containment control for nonlinear multi-agent systems with external disturbances[J]. IEEE Transactions on Circuits and Systems II: Express Briefs, 2022, 69(2): 459-463.

[5] Zhang F X, Chen Y Y. Fuzzy adaptive containment control for nonlinear nonaffine pure-feedback multiagent systems[J]. IEEE Transactions on Fuzzy Systems, 2021, 29(10): 2878-2889.

[6] Li Y M, Qu F Y, Tong S C. Observer-based fuzzy adaptive finite-time containment control of nonlinear multiagent systems with input delay[J]. IEEE Transactions on Cybernetics, 2021, 51(1): 126-137.

[7] Cheng W L, Zhang K, Jiang B, et al. Fixed-time fault-tolerant formation control for heterogeneous multi-agent systems with parameter uncertainties and disturbances[J]. IEEE Transactions on Circuits and Systems I: Regular Papers, 2021, 68(5): 2121-2133.

[8] 苏博, 王洪斌, 王跃灵, 等. 基于固定时间滑模干扰观测器的AUVs事件触发编队控制[J]. 控制与决策, 2022, 37(5): 1116-1126.
(Su B, Wang H B, Wang Y L, et al. Event-triggered formation control for AUVs with fixed-time sliding mode disturbance observer[J]. Control and Decision, 2022, 37(5): 1116-1126.)

[9] Cai G B, Zhao Y S, Zhao Y, et al. Consensus of multi-vehicle cooperative attack with stochastic multi-hop time-varying delay and actuator fault[J]. Journal of Systems Engineering and Electronics, 2021, 32(1): 228-242.

[10] Dai Z J, Zhang Y, Zhang W C, et al. A multi-agent

collaborative environment learning method for UAV deployment and resource allocation[J]. IEEE Transactions on Signal and Information Processing Over Networks, 2022, 8: 120-130.
[11] Lin G H, Li H Y, Ahn C K, et al. Event-based finite-time neural control for human-in-the-loop UAV attitude systems[J]. IEEE Transactions on Neural Networks and Learning Systems, DOI: 10.1109/TNNLS.2022.3166531.
[12] Ma H, Zhou Q, Li H Y, et al. Adaptive prescribed performance control of a flexible-joint robotic manipulator with dynamic uncertainties[J]. IEEE Transactions on Cybernetics, DOI: 10.1109/TCYB.2021.3091531.
[13] Zhu J W, Gu C Y, Ding S X, et al. A new observer-based cooperative fault-tolerant tracking control method with application to networked multiaxis motion control system[J]. IEEE Transactions on Industrial Electronics, 2021, 68(8): 7422-7432.
[14] You X, Hua C C, Yu H N, et al. Leader-following consensus for high-order stochastic multi-agent systems via dynamic output feedback control[J]. Automatica, 2019, 107: 418-424.
[15] Wang F, Chen B, Lin C, et al. Distributed adaptive neural control for stochastic nonlinear multiagent systems[J]. IEEE Transactions on Cybernetics, 2017, 47(7): 1795-1803.
[16] Wu Y, Pan Y N, Chen M, et al. Quantized adaptive finite-time bipartite NN tracking control for stochastic multiagent systems[J]. IEEE Transactions on Cybernetics, 2021, 51(6): 2870-2881.
[17] 郑晓宏, 董国伟, 周琪, 等. 带有输出约束条件的随机多智能体系统容错控制[J]. 控制理论与应用, 2020, 37(5): 961-968.
(Zheng X H, Dong G W, Zhou Q, et al. Fault-tolerant control for stochastic multi-agent systems with output constraints[J]. Control Theory & Applications, 2020, 37(5): 961-968.)
[18] Lan J, Liu Y J, Liu L, et al. Adaptive output feedback tracking control for a class of nonlinear time-varying state constrained systems with fuzzy dead-zone input[J]. IEEE Transactions on Fuzzy Systems, 2020, 29(7): 1841-1852.
[19] 周琪, 林国怀, 马慧, 等. 输入死区下的多输入多输出系统自适应神经网络容错控制[J]. 中国科学: 信息科学, 2021, 51(4): 618-632.
(Zhou Q, Lin G H, Ma H, et al. Adaptive neural network fault-tolerant control for MIMO systems with dead zone inputs[J]. Scientia Sinica: Informationis, 2021, 51(4): 618-632.)
[20] Li S, Ding L, Gao H B, et al. Adaptive fuzzy finite-time tracking control for nonstrict full states constrained nonlinear system with coupled dead-zone input[J]. IEEE Transactions on Cybernetics, 2022, 52(2): 1138-1149.
[21] Ma J L, Wang J Q, Fei S M, et al. Global fixed-time control for nonlinear systems with unknown control coefficients and dead-zone input[J]. IEEE Transactions on Circuits and Systems II: Express Briefs, 2022, 69(2): 594-598.
[22] Ma H, Ren H R, Zhou Q, et al. Approximation-based nussbaum gain adaptive control of nonlinear systems with periodic disturbances[J]. IEEE Transactions on Systems, Man, and Cybernetics: Systems, 2022, 52(4): 2591-2600.
[23] Dong G W, Li H Y, Ma H, et al. Finite-time consensus tracking neural network FTC of multi-agent systems[J]. IEEE Transactions on Neural Networks and Learning Systems, 2020, 32(2): 653-662.
[24] Ma Z Y, Ma H J. Improved adaptive fuzzy output-feedback dynamic surface control of nonlinear systems with unknown dead-zone output[J]. IEEE Transactions on Fuzzy Systems, 2021, 29(8): 2122-2131.
[25] Huang Y, Jia Y M. Adaptive finite-time 6-DOF tracking control for spacecraft fly around with input saturation and state constraints[J]. IEEE Transactions on Aerospace and Electronic Systems, 2019, 55(6): 3259-3272.
[26] Cao L, Li H Y, Dong G W, et al. Event-triggered control for multiagent systems with sensor faults and input saturation[J]. IEEE Transactions on Systems, Man, and Cybernetics: Systems, 2021, 51(6): 3855-3866.
[27] 周琪, 陈广登, 鲁仁全, 等. 基于干扰观测器的输入饱和多智能体系统事件触发控制[J]. 中国科学: 信息科学, 2019, 49(11): 1502-1516.
(Zhou Q, Chen G D, Lu R Q, et al. Disturbance-observer-based event-triggered control for multi-agent systems with input saturation[J]. Scientia Sinica: Informationis, 2019, 49(11): 1502-1516.)
[28] Wang L J, Chen C L P. Reduced-order observer-based dynamic event-triggered adaptive NN control for stochastic nonlinear systems subject to unknown input saturation[J]. IEEE Transactions on Neural Networks and Learning Systems, 2021, 32(4): 1678-1690.
[29] Min H F, Xu S Y, Zhang Z Q. Adaptive finite-time stabilization of stochastic nonlinear systems subject to full-state constraints and input saturation[J]. IEEE Transactions on Automatic Control, 2021, 66(3): 1306-1313.

作者简介

于跃飞 (1996–), 男, 硕士生, 从事多智能体系统控制、自适应神经网络控制等研究, E-mail: gdut_yyf@163.com;

林国怀 (1995–), 男, 博士生, 从事多智能体系统协同控制、人在回路控制和自适应神经网络控制等研究, E-mail: linguohuai2019@163.com;

马慧 (1994–), 女, 博士后, 从事自适应控制、模糊控制和事件触发控制等研究, E-mail: huima2016@163.com;

周琪 (1983–), 女, 教授, 博士生导师, 从事网络化控制系统、鲁棒控制等研究, E-mail: zhouqi2009@gmail.com;

鲁仁全 (1971–), 男, 教授, 博士生导师, 从事复杂系统、 网络化控制系统和非线性系统等研究, E-mail: lurenquan2012@163.com.

(责任编辑: 魏 冰)